Insight into the Raman shifts and optical absorption changes upon annealing polymer/fullerene solar cells

Je-Jung Yun,[1,2,a)] Jeffrey Peet,[1,2] Nam-Sung Cho,[1,2] Guillermo C. Bazan,[1,2] Seung Joon Lee,[1] and Martin Moskovits[1]
[1]*Department of Chemistry and Biochemistry, University of California, Santa Barbara, California 93106, USA*
[2]*Institute of Polymers and Organic Solids, University of California at Santa Barbara, Santa Barbara, California 93106-5096, USA*

(Received 28 January 2008; accepted 3 May 2008; published online 27 June 2008)

Raman shifts and optical absorption spectra of bulk heterojunction films were measured to elucidate the origin of the optimum annealing parameters. A series of device optimization studies revealed 413 K to be the optimum annealing temperature, leading to a power conversion efficiency of 2.95%. The highest power conversion efficiency coincides with the highest peak in the UV-visible absorption and the lowest full width at half maximum of the —C═C— symmetric stretching signal in the Raman spectra. The changes observed in the vibronic shifts could be useful in obtaining information about the optimal performance and processing conditions for polymer optoelectronic devices. © *2008 American Institute of Physics*. [DOI: 10.1063/1.2940205]

Poly (3-hexylthiophene) (P3HT) based organic solar cells have been intensely studied due to strong absorption in the visible spectrum and a high degree of intermolecular order leading to a relatively high hole mobility of $\sim 0.1\ cm^2\ V^{-1}\ s^{-1}$.[1–4] [6,6]-penyl-$C_{61}$ butyric acid methyl ester (PCBM) has been shown to be uniquely effective as the electron acceptor in polymer bulk heterojunction (BHJ) solar cells. The P3HT/PCBM combination has dominated the field of polymer-based solar cells for some time and is very well characterized, at least in comparison to other BHJ systems.[5–7] As in other organic semiconducting devices, solar cell performance is strongly influenced by processing conditions. While several methods are available for manipulating the BHJ morphology, thermal annealing is generally accepted as the standard technique for optimizing BHJ devices which use a semicrystalline polymer as the electron donor material in the active layer.[8,11] Reaching the optimal annealing time and temperature is typically achieved empirically, as the effects of annealing on donor/acceptor phase separation and polymer crystallization are difficult to deconvolute.[1,5,9] P3HT crystallization upon annealing has been shown to increase carrier mobility as well as optical absorption and vibronic definition; however, thermal annealing at higher than optimum temperatures or for long periods of time leads to large scale polymer/fullerene phase separation.[3,9–12] Several reports highlight the increased solar power conversion efficiency observed upon thermal annealing (η_{eff}, 2.7–5.0) yet the process by which the internal order of the active layer evolves and the resulting final organization within the BHJ remain poorly understood.[2,3,5,9–14]

Conjugated polymers generally show Raman shifts that correspond with the degree of π-electron delocalization along the chain axis.[15–18] Raman spectroscopy has also been shown to be a useful tool for monitoring nanoscale changes in morphology by monitoring the vibrational modes associated with the portions of the polymer chains involved in electronic transitions.[17,19–22] In this contribution, we show that Raman spectroscopy can be used to monitor changes in the local polymer order as a function of thermal treatment and that the resulting signals correlate with optimal device performance.

Solar cell devices were fabricated on corning 1737 glass patterned with 140 nm thick indium tin oxide (ITO) (Φ =4.2 eV) by Thin Film Devices, Inc. As a 50 nm buffer layer, optically transparent conducting poly(ethylenedioxythiphene):poly(styrene sulfonic acid) (PEDOT:PSS) (Baytron P, HC Stark) was spun cast (5000 rpm) and then dried at 413 K for 15 min in air. The photoactive layer of P3HT (Rieke metals, EE grade) and PCBM (Nano-C) was spun cast onto the buffer layer at 700 rpm (film thickness $\sim$100 nm by atomic force microscopy) using a 0.45 μm Whatman syringe filter. Chlorobenzene was used to dissolve the P3HT and PCBM due to its relatively high boiling point. The weight ratio of the P3HT/PCBM was 5:4 with P3HT dissolved at 10 mg/mL. Films were thermally annealed on a digital hotplate for 10 min in a nitrogen glovebox. For current-voltage measurements, an 80 nm Al (Φ=4.7 eV) cathode was deposited by thermal evaporation of high purity Al metal (99.999%, Sigma Aldrich) at a deposition rate of less than 0.5 nm/s with chamber pressure of less than 2×10^{-6} torr.

Device efficiencies were measured using a 150 W Newport–Oriel Xe light source calibrated to simulate 100 mW/cm^2 of AM 1.5 global illumination. The illumination intensity was calibrated using a monocrystalline silicon cell calibrated at the National Renewable Energy Laboratory (NREL) with a KG5 color glass filter. Incident photon conversion efficiency (IPCE) spectra were measured with a Spectral Products CM110 monochromator underfilling the device active area. The IPCEs integrate to the obtained short circuit current values based on the ASTM reference 100 mW/cm^2 AM 1.5 global spectrum.[23] The photocurrent was obtained from a calibrated Newport–Oriel photodiode with a Keithley 2602 source/measure unit.

[a)]Author to whom correspondence should be addressed. Present address: Business supporting team, Jeonnam Nanobio Center, 1063-50, Yeongcheon-ri, Jangseong-gun, Jeollanam-do, Korea, 515-806. Electronic mail: solartopphd@yahoo.com.

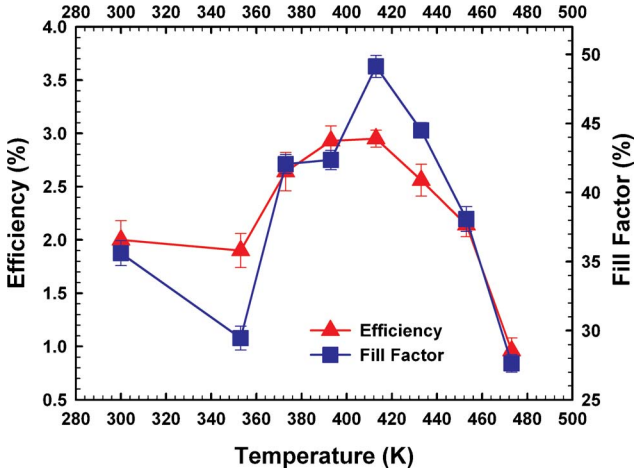

FIG. 1. (Color online) Fill factors and power conversion efficiency are shown as a function of annealing temperature under simulated 100 mW/cm^2 AM 1.5 G illumination.

Backscattered Raman spectra were recorded on a LabRam micro-Raman system (Jobin–Yvon/ISA) equipped with a thermoelectrically cooled charge-coupled device. The spectra were excited using the 514.5 nm line of a continuous wave Ar ion laser (SpectraPhysics 164). The incident laser beam was focused to a beam size of 1 μm, and the Raman signal was collected using a 100× objective with a numerical aperture of 0.8. Approximately 0.7 mW of laser irradiation was used to excite the samples. The signal collection time was 30 s. For the purpose of the Raman and UV-visible absorption spectra, the structure was consisted of ITO (~140 nm)/PEDOT:PSS(~50 nm)/P3HT:PCBM(~100 nm).

Figure 1 shows the power conversion efficiencies and fill factors for each device (ITO/PEDOT:PSS/P3HT:PCBM/Al) along with the corresponding annealing temperature. The highest power conversion efficiency of 2.95% and a fill factor of 49% were obtained by annealing at 413 K for 10 min. Because the internal P3HT ordering and the phase separation of the polymer and fullerene domains are nonoptimal after spin casting, altering the morphology via thermal annealing or another technique is critical for achieving high performance solar cells. The IPCE measurements indicate that the annealing temperature has an important effect on device performance. Devices annealed at 353, 373, 393, and 413 K for 10 min yield over 50% quantum efficiency and show increased carrier generation from the vibronic portion of the P3HT absorption near 600 nm.

Figure 2 shows the changes in the Raman spectra from P3HT:PCBM films as a function of annealing temperature. Figure 2(a) shows the increase in the Raman shift (1560–1350 cm^{-1}) with annealing temperature. The weakest Raman shift is associated with the 413 K annealed devices. The peaks at 1454–1450 and 1380 cm^{-1} are attributed to the —C═C— symmetric stretching ($\nu_{C=C}$) and the —C—C— skeletal stretching of the thiophene ring, respectively.[1,17,20,21] Since the thiophene rings are, on average, more closely stacked when the polymer is highly crystalline, the increased crystallite size and better internal order within the P3HT domains obtained with annealing leads to narrowing and overall weakening in the $\nu_{C=C}$.[1,17,19–22] Possible interference in the $\nu_{C=C}$ peak from PCBM or PEDOT:PSS was ruled out because of the low intensity signals observed for pristine PCBM and PEDOT:PSS samples. Thus, the characteristics of

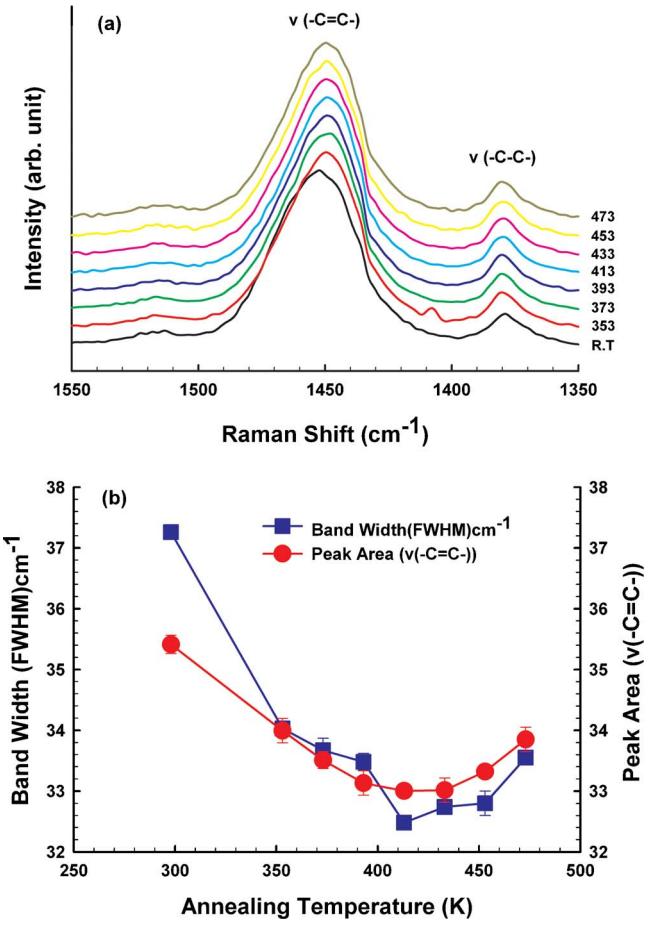

FIG. 2. (Color online) (a) The increase in the Raman spectra for P3HT/fullerene devices with the corresponding $\nu_{—C=C—}$ (1560–1350 cm^{-1}) as a function of the annealing temperature.(b) The peak areas and FWHM of the carbon double bond of P3HT/fullerene devices with the annealing temperatures. (a) and (b) are from the 1400–1505 cm^{-1} peak.

the $\nu_{C=C}$ band correlate with changes in the P3HT conformation, conjugation length, and nanostructure.

A minima of 33.0 (arbitrary units) $\nu_{C=C}$ peak area is observed for the film that was annealed at 413 K in Fig. 2(b) and the largest area (35.4 a.u.) corresponds to the films that were not annealed. The effect of thermal annealing on the full width at half maximum (FWHM) of the $\nu_{C=C}$ Raman band is shown in Fig. 2(b). A minimum is observed for the sample heated to 413 K. The difference between the lowest and highest value for the FWHM is ~5 cm^{-1}.

The changes in the Raman spectra correlate with changes in the absorption bands of P3HT:PCBM for films annealed at the same temperatures. Figure 3(a) shows the progression of the optical absorption spectra as a function of the annealing temperature.[24] The primary absorption peak at 550 nm reaches a maximum at 413 K, coinciding with the maximum device efficiency and minimum $\nu_{C=C}$ peak area and FWHM. These results are well matched with the ratio of the Ω_{shunt} to the Ω_{series}, which increases from 97.2 at 353 K to 4938.6 at 413 K and decreases to 1382 at 433 K as illustrated in Fig. 3(b). The Ω_{shunt} and Ω_{series} are characteristic resistances. The higher the ratio of the shunt resistance to the series resistance, the closer the diode is to ideality. On the basis of these results, annealing at this temperature may lead to a more ordered P3HT. Additional increases in annealing temperature likely lead to an unfavorable degree of phase separation between the P3HT and PCBM domains. These

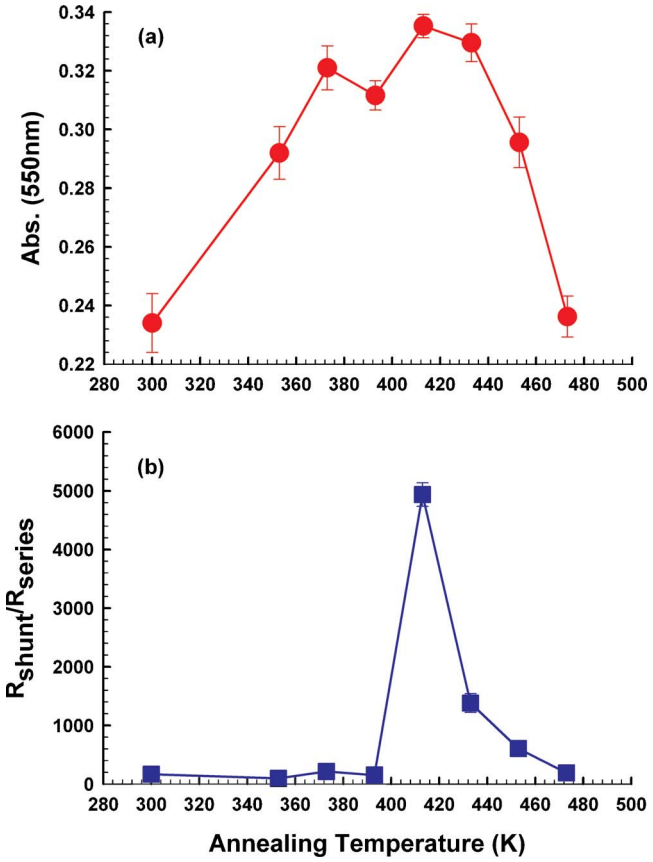

FIG. 3. (Color online) (a) UV-visible absorption spectra show the progression of the primary absorption peak at 550 nm as a function of the annealing temperature. (b) The ratio of Ω_{shunt} to Ω_{series} for devices measured in the dark.

phenomena can be inferred from the reduced band gap which is related to the P3HT π-electron delocalization and can be monitored by the redshift in the optical absorption. While the absorption redshift increases with annealing temperatures above 413 K, increased phase separation likely leads to decreased device performance.

In summary, the work described herein shows that the Raman shifts of the P3HT in BHJ active layers can provide diagnostic signals that give insight into the polymer solar cell nanostructure. Annealing at 413 K can lead to increased IPCE owing to the optimal nanostructure of the active layer. These results relate the increased delocalization of the π-electrons in P3HT annealed at 413 K with the best structure for photovoltaic applications. We have discovered that by measuring the Raman spectra and UV-visible absorption spectra, one can obtain features that correlate with the internal order in polymer BHJ solar cells. In the future, the analysis of Raman spectra changes, photovoltaic effects, and UV-visible absorption spectra of conjugated polymers may be a useful tool to obtain information about the internal order of blended polymer devices. Additionally, insight into the vibronic shifts may be used to provide a simplified method for finding the ideal set of processing parameters for optimal performance.

This work was supported by the Korea Research Foundation Grant funded by the Korean Government (MOEHRD) (KRF-2006-214-D00030). G.C. Bazan acknowledges Office of Naval Research, USA.

[1]E. Klimov, W. Li, X. Yang, G. G. Hoffmann, and J. Loos, Macromolecules **39**, 4493 (2006).
[2]H. Sirringhaus, P. J. Brown, R. H. Friend, M. M. Nielsen, K. Bechaard, B. M. W. Langeveld-Voss, A. J. H. Spiering, R. A. J. Janssen, E. W. Meijer, P. Herwig, and D. M. de Leeuw, Nature (London) **401**, 685 (1999).
[3]Y.-G. Kim, S. Cook, S. M. Tuladhar, S. A. Choulis, J. Nelson, J. Durrant, D. D. C. Bradley, M. Giles, I. Mcculloch, C.-S. Ha, and M.-H. Ree, Nat. Mater. **5**, 197 (2006).
[4]G. Wang, J. Swensen, D. Moses, and A. J. Heeger, J. Appl. Phys. **93**, 6137 (2003).
[5]R. Cugola, U. Giovanella, P. D. Gianvincenzo, F. Bertini, M. Catellani, and S. Luzzati, Thin Solid Films **511**, 489 (2006).
[6]I. Riedel and V. Dyakonov, Phys. Status Solidi A **6**, 1332 (2004).
[7]G. Yu, J. Gao, J. C. Hemmelen, F. Wudl, and A. J. Heeger, Science **270**, 1789 (1995).
[8]J. Peet, C. Soci, R. C. Coffin, T. Q. Nguyen, A. Mikhailovsky, D. Moses, and G. C. Bazan, Appl. Phys. Lett. **89**, 252105 (2006).
[9]T. Erb, U. Zhokhavets, G. Gobsch, S. Raleva, B. Stühn, P. Schilinsky, C. Waldauf, and C. J. Brabec, Adv. Funct. Mater. **15**, 1193 (2005).
[10]S. W. Cho, J. H. Seo, C. Y. Kim, K.-H. Yoo, K. Jeong, and C.-N. Whang, Appl. Phys. Lett. **88**, 151103 (2006).
[11]G. Li, V. Shrotriya, J. Huang, Y. Yao, T. Moriarty, K. Emery, and Y. Yang, Nat. Mater. **4**, 864 (2005).
[12]V. Dyakonov, Appl. Phys. A: Mater. Sci. Process. **79**, 21 (2004).
[13]J.-J. Yun, H.-S. Jung, S.-H. Kim, V. Vaithianathan, S. A. Jenekhe, and E.-M. Han, Appl. Phys. Lett. **88**, 123102 (2006).
[14]P. J. Brown, D. S. Thomas, A. Kohler, J. S. Wilson, J.-S. Kim, C. M. Ramsdale, H. Sirringhaus, and R. H. Friend, Phys. Rev. B **67**, 064203 (2003).
[15]V. Hernandez, S. C. Losada, J. Casado, H. Higuchi, and J. T. L. Navarrete, J. Phys. Chem. A **104**, 661 (2000).
[16]S. Masubuchi and S. Kazama, Synth. Met. **74**, 151 (1995).
[17]J. Casado, R. G. Hicks, V. Hernandez, D. J. T. Myles, M. C. R. Delgado, and J. T. L. Navarrete, J. Chem. Phys. **118**, 1912 (2003).
[18]V. Hernandez, C. Castiglioni, M. D. Zoppo, and G. Zerbi, Phys. Rev. B **50**, 9815 (1994).
[19]Z. Liao and J. E. Pemberton, J. Phys. Chem. A **110**, 13744 (2006).
[20]Y. W. Goh, Y. F. Lu, Z. M. Rem, and T. C. Chong, Appl. Phys. A: Mater. Sci. Process. **77**, 433 (2003).
[21]P. S. O. Patrico, H. D. R. Calado, F. A. C. de Oliveira, A. Righi, B. R. A. Neves, G. G. Silva, and L. A. Cury, J. Phys.: Condens. Matter **18**, 7529 (2006).
[22]M. Sridharan, M. Mekaladevi, S. K. Narayandass, D. Mangalaraj, and H. C. Lee, Cryst. Res. Technol. **4**, 328 (2004).
[23]ASTM G-173-03, ASTM International, West Conshohocken.
[24]P. Vanlaeke, A. Swinnen, I. Haeldermans, G. Vanhoyland, T. Aernouts, D. Cheyns, C. Deibel, J. D'Haen, P. Heremans, J. Poortmans, and J. V. Manca, Sol. Energy Mater. Sol. Cells **90**, 2150 (2006).